Proceedings of the 11th
KACC, October 1996

SWITCHED-VOLTAGE CONTROL OF ELECTROSTATIC SUSPENSION SYSTEM

°Shao Jü Woo*, Jong Up Jeon*, and Toshiro Higuchi*,**

*Kanagawa Academy of Science and Technology, East Block 405, KSP, 3-2-1 Sakado, Takatsu-ku, Kawasaki 213, JAPAN
Tel: +81-44-819-2093; Fax: +81-44-819-2095; E-mail: woo%naeba@intellect.pe.u-tokyo.ac.jp

**Dept. of Precision Machinery Eng., The University of Tokyo, 7-3-1 Hongo, Bunkyo-ku, Tokyo 113, JAPAN
Tel:+81-3-3812-2111 ext. 6449; Fax:+81-3-5800-6968; E-mail: higuchi@intellect.pe.u-tokyo.ac.jp

Abstract A new method for the electrostatic suspension of disk-shaped objects is proposed which is based on a switched-voltage control scheme. It operates according to a relay feedback control and deploys only a single high-voltage power supply capable of delivering a dc voltage of positive and/or negative polarity. In addition to the unique feature that no high-voltage amplifiers are needed, this method provides a remarkable system simplification relative to conventional methods. It is shown that despite the inherent limit cycle property of relay feedback based control, an excellent performance in vibration suppression is attained due to the presence of a relatively large squeeze film damping.

In this paper, the functional principle of the switched voltage control scheme, numerical analysis, stator electrode design, and a nonlinear dynamic model of the suspension system are described. Experimental results will be presented for a 4-inch silicon wafer that clearly reveal the capability of the proposed control structure to suspend the wafer stably at an airgap length of 50 μm.

Keywords Switched-Voltage Control, Electrostatic Suspension, 4-inch Silicon Wafer Suspension

1. INTRODUCTION

Electrostatic suspension offers the advantage to directly suspend various materials without any mechanical contact, such as conductive materials, semiconductors and dielectric materials. This is in contrast to electromagnetic suspension which can only suspend ferro-magnetic materials. However, both types of suspension techniques require feedback control to stabilize the suspended object's position and attitude. The use of actively controlled electrostatic forces has been applied to suspend disk-shaped objects, such as silicon wafers [1], aluminum hard disk media [2], and glass plates [3-4]. In order to obtain sufficient large electric suspension forces, the stator electrodes acting as the force actuators are supplied with high voltages. Conventional electrostatic suspension systems utilize high-voltage amplifiers in a PID based feedback control scheme to generate these high voltages. However, a major disadvantage of these systems is that the high-voltage amplifiers are relatively costly and bulky system components which are critical factors determining potential industrial application. Clearly, the number of high-voltage amplifiers are proportional to the number of individual stator electrodes to be controlled. This would result in extreme system costs in the case of distributed electrode patterns used for the suspension of large flexible objects.

In this paper, a switched-voltage control scheme, that operates according to a relay feedback control, is proposed for the electrostatic suspension of objects having a large surfacial area/thickness ratio. This method has the inherent property that it does not deploy any high-voltage amplifiers. Instead only a single high-voltage power supply is required that can deliver a constant voltage of positive and/or negative polarity for an arbitrary number of individual stator electrodes that have to be controlled.

The feasibility of stable suspension is ensured by the relatively large nonlinear squeeze air film damping produced by the relative axial or tilting motion of the levitated object with respect to the electrodes. Despite the introduction of limit cycles which are inherent to relay feedback based control, a good performance in vibration suppression can be obtained as a result of the squeeze film damping. In addition, due to the on/off nature of the controller, the requirements for the airgap sensors can be less strict. Proximity type of sensors are sufficient to accomplish stable levitation. Therefore, the proposed method provides major improvements from economic, weight, space, and reliability points of view. Experimental validation of the proposed scheme has been performed through the successful suspension of a 4-inch silicon wafer.

2. PRINCIPLE OF OPERATION

The basic principle of the proposed method is clarified on the basis of an one-degree of freedom electrostatic suspension system

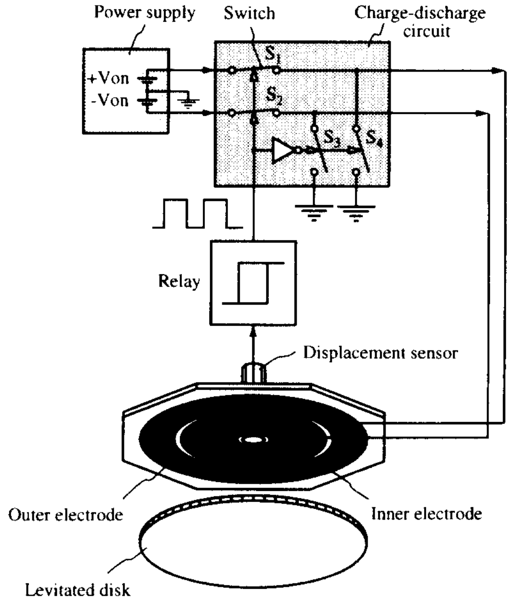

Fig. 1. One DOF electrostatic suspension system employing switched voltage control.

as shown in Fig. 1. The 1-DOF system employs two concentric electrodes which are supplied with a voltage of positive ($+V_{on}$) and negative polarity ($-V_{on}$), respectively. By configuring both electrodes to have the same surfacial areas, the electric potential of the levitated object will become zero volt. In case of silicon wafers, a zero volt potential is imperative to prevent wafer surface contamination through the attraction of particulates. Each stator electrode forms a variable capacitor with the suspended object where the airgap is much smaller than the area of the electrode overlapping with the suspended object. The position of the levitated object is measured using an airgap sensor and is fed to a relay incorporating hysteresis that operates as a nonlinear controller. Based on the measured position signal, the variable capacitors are either simultaneously being charged through the switches S_1 and S_2 or discharged through the switches S_3 and S_4.

The switched-voltage control scheme imposes through it's on/off action a persistent oscillation on the levitated object in the form of a limit cycle. The amplitude of this oscillation is a function of the charging voltage, hysteresis, and airgap. Particularly, the nonlinear squeeze air film damping plays a pivotal role in suppressing the limit cycle vibration of the suspended object since its magnitude is of the same order as the electric suspension force.

3. DYNAMIC MODEL AND SIMULATION

3.1 Systems Modeling

The systems model of the 1-DOF suspension system will be derived using its electrical circuit representation as shown in Fig. 2.

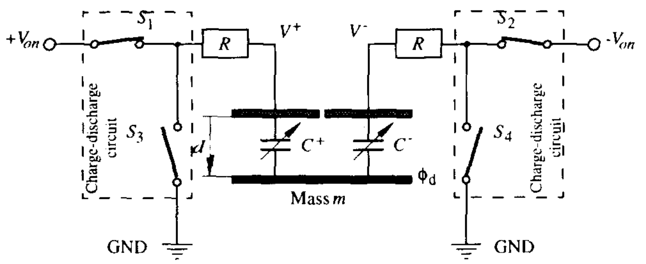

Fig. 2. Electrical circuit representation of one-DOF electrostatic suspension system: R represents the electric resistance of the switches S_1, S_2, S_3 and S_4 in on-state and that of the cables connecting the power supplies $+V_{on}$ and $-V_{on}$ to the electrodes. The mass of the disk is denoted as m while d denotes the airgap length between the disk and the electrodes. C^+ and C^- represent the variable capacitors formed by the disk and the positively and negatively charged electrode respectively.

As an electromechanical system, the open-loop dynamical model of the suspension system is formed by the coupled dynamical equations of the disk, which constitutes the mechanical subsystem, and the electrical subsystem.

3.1.1 Mechanical Subsystem

The various forces acting on the suspended disk are the squeeze film damping, attractive electric, gravitational, and external disturbance force. The squeeze film damping force can be found by solving the Reynolds equations for incompressible media yielding the following time varying pressure distribution under the electrode:

$$p(r,t) = \frac{3\eta(r^2 - r_d^2)}{d^3}\frac{\partial d}{\partial t} \tag{1}$$

where: $\eta = 18 \cdot 10^{-6}$ Nsec/m^2 is the viscosity of ambient air, r is the polar coordinate with respect to an inertial frame whose origin is located in the geometrical center of the stator, and r_d represents the radius of the disk. Subsequently, the nonlinear squeeze film damping force exerted on the disk can be obtained by an integration of (1) over the area of the disk.

$$F_s(d,t) = \int_{r=0}^{r=r_d} p(r,t)2\pi r dr = \frac{3\pi\eta r_d^4}{2d^3}\frac{\partial d}{\partial t} \tag{2}$$

The attractive electric force can be found from:

$$\left|F_e(V^+,V^-,d)\right| = \left|\frac{\partial W_e(V^+,V^-,d)}{\partial d}\right| \tag{3}$$

where: W_e is the electric field energy stored by the variable capacitors C^+ and C^- and is given by:

$$W_e(V^+,V^-,d) = \frac{1}{2}\frac{C^+C^-}{C^+ + C^-}(V^+ - V^-)^2 \tag{4}$$

The assumption of an uniform electric field between the disk and the electrodes is allowed since the airgap is much smaller than the surfacial area of the disk. This leads to the following relation for the attractive electric force:

$$\left|F_e(V^+,V^-,d,t)\right| = \frac{1}{2}\frac{\varepsilon A^+A^-(V^+-V^-)}{d(A^++A^-)}\left|2\frac{\partial(V^+-V^-)}{\partial t}\Big/\frac{\partial d}{\partial t} - \frac{(V^+-V^-)}{d}\right| \tag{5}$$

where $\varepsilon = 8.85971 \cdot 10^{-12}$ farad/m represents the permittivity of air and A^+ and A^- denote the area of the positively and negatively charged electrodes, respectively. Using (2) and (5), the nonlinear equation of motion of the disk can be written as:

$$m\frac{\partial^2 d}{\partial t^2} = mg - F_s(d,t) - \left|F_e(V^+,V^-,d,t)\right| + F_d \tag{6}$$

where F_d denotes the external disturbance force.

3.1.2 Electrical Subsystem

The charging-discharging dynamics of the electrical subsystem is governed by:

$$V_{on} = \frac{R\varepsilon A^+A^-}{d(A^++A^-)}\frac{\partial(V^+-V^-)}{\partial t} + (V^+-V^-)\left(\frac{1}{2} - \frac{R\varepsilon A^+A^-}{d^2(A^++A^-)}\frac{\partial d}{\partial t}\right) \tag{7}$$

3.1.3 State-space Model of Open-loop System

A nonlinear state-space representation of the open-loop system can be derived on the basis of Eqs. (6) and (7) as:

$$\begin{aligned} \dot{x}_1 &= x_2 \\ \dot{x}_2 &= g - \theta_1\frac{x_2}{x_1^3} - \theta_2\frac{x_3^2}{x_1^2}\left|2\frac{x_1}{x_2}\frac{\dot{x}_3}{x_3} - 1\right| + \frac{F_d}{m} \\ \dot{x}_3 &= \theta_3 x_1\left(u - x_3\left(\frac{1}{2} - \theta_4\frac{x_2}{x_1^2}\right)\right) \end{aligned} \tag{8}$$

where: $x_1 = d$, $x_3 = V^+ - V^-$, $u = V_{on}$, $\theta_1 = \frac{3\pi\eta R_d^4}{2m}$, $\theta_2 = \frac{\varepsilon A^+A^-}{2m(A^++A^-)}$, $\theta_3 = \theta_4^{-1}$, and $\theta_4 = \frac{R\varepsilon A^+A^-}{(A^++A^-)}$.

The usual linearization of the dynamical equations cannot be performed since, for practical values of R, only the state variables x_1 and x_2 exhibit an oscillational behavior around the nominal position d_n that is small enough to allow for a linearization.

3.2 Simulation Results

The 1-DOF system depicted in Fig. 1 is subjected to a simulation study using the state-space model (8). The system parameters employed for the simulation are listed in Table 1. The reference airgap

Table 1. Simulation parameters.

parameter	unit	value
r_d	m	0.05
A^+	m^2	$3.927 \cdot 10^{-3}$
A^-	m^2	$3.927 \cdot 10^{-3}$
R	Ω	500
m	kg	$9 \cdot 10^{-3}$
θ_1	m^3/s	$5.8905 \cdot 10^{-8}$
θ_2	m^3/V^2s^2	$9.6645 \cdot 10^{-13}$
θ_3	$m^{-1}s^{-1}$	$1.149686 \cdot 10^{11}$
θ_4	ms	$8.698 \cdot 10^{-12}$

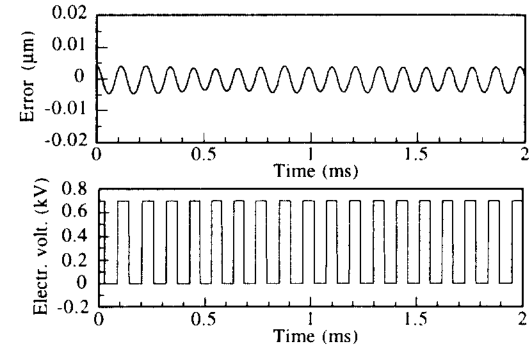

Fig. 3. Simulated steady-state position error and electrode voltage.

length was set at 300 μm and a charging voltage V_{on} of 700 V was utilized. A hysteresis band of zero was used for the relay. Fig. 3 shows the simulated time functions of the position variation from the reference airgap and the electrode voltage V^+ in steady-state. As evidenced from Fig. 3, the suspended disk's position exhibits a stable limit cycle around the reference airgap and has a very small amplitude.

4. EXPERIMENTAL SYSTEM

4.1 *Stator Electrode Pattern Design*

Fig. 4 shows the electrode pattern which was designed to suspend a 4-inch silicon wafer. Fig. 5 depicts a photograph of the stator. The stator electrode consists of three segment electrode units

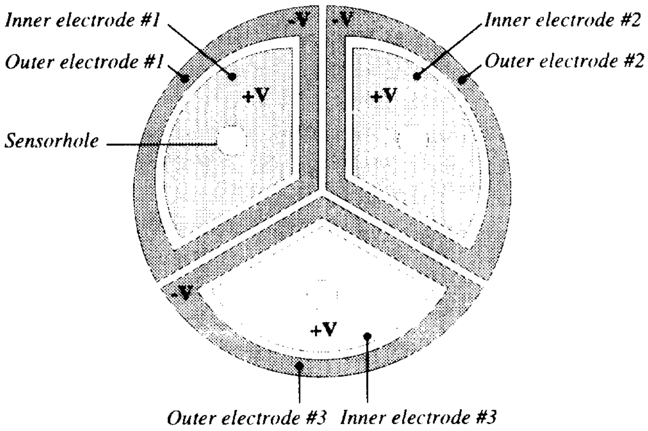

Fig. 4. Stator electrode pattern with charging voltage distribution.

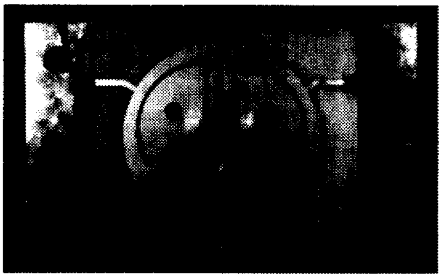

Fig. 5. Photograph of stator electrode.

equally arranged to be circumscribed by a circle with the same diameter as the wafer. The surfacial area of one unit measures 22.84 cm^2. Each unit constitutes an independent electrostatic force actuator and is a combination of an outer and inner electrode segment whose areas are the same. As aforementioned, this geometry is required to guarantee a wafer potential near to zero volt during the suspension process. The sensor sites lie on a circle having a diameter of 55.48 mm and are colocated with the geometrical centers of the electrode units. Using this pattern, three degrees of freedom can be actively controlled, namely vertical motion and roll and pitch angle. The remaining degrees of freedom, among which the longitudinal and lateral translations, are passively stabilized through electrostatic restriction forces [5].

4.2 *Experimental Apparatus*

A highly compact switching controller circuit incorporating the charge-discharge circuits and feedback relays was constructed. Fig. 6 shows a photograph of the controller and the mechanical setup.

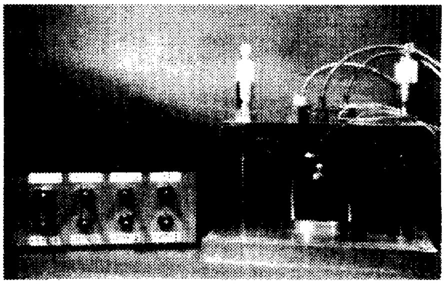

Fig. 6. Photograph of suspension system.

The stator electrode can be leveled using micrometer screws while the silicon wafer is supported below the stator by three micrometer screws. Fabrication of the copper made stator electrodes was performed using a wet chemical etching process. As airgap sensors, three optical fiber sensors were utilized.

4.3 *Control Strategy*

The control strategy is based on assigning independent switched-voltage controllers to each electrode unit. Each of these controllers use the local airgap length measured by the corresponding gap sensor as input signal for the feedback relays. This approach basically leads to a decentralized control structure which contributes to a further simplification of the controller hardware.

5. EXPERIMENTS AND DISCUSSION

The object to be suspended was a 4-inch silicon wafer having a mass of approximately 9 g. The experimental conditions were as follows:

(1) The hysteresis band of the relays were set to zero; this corresponds to operating the switched-voltage controllers in Bang Bang control mode;

(2) The reference and initial airgap were set at 50 μm and 70 μm, respectively;

(3) A dc charging voltage of positive and negative polarity, having a level of +180 V and -180 V, respectively, were supplied to each of the three electrode units using a high-voltage power supply.

Fig. 7 shows the recorded airgap deviations from the reference

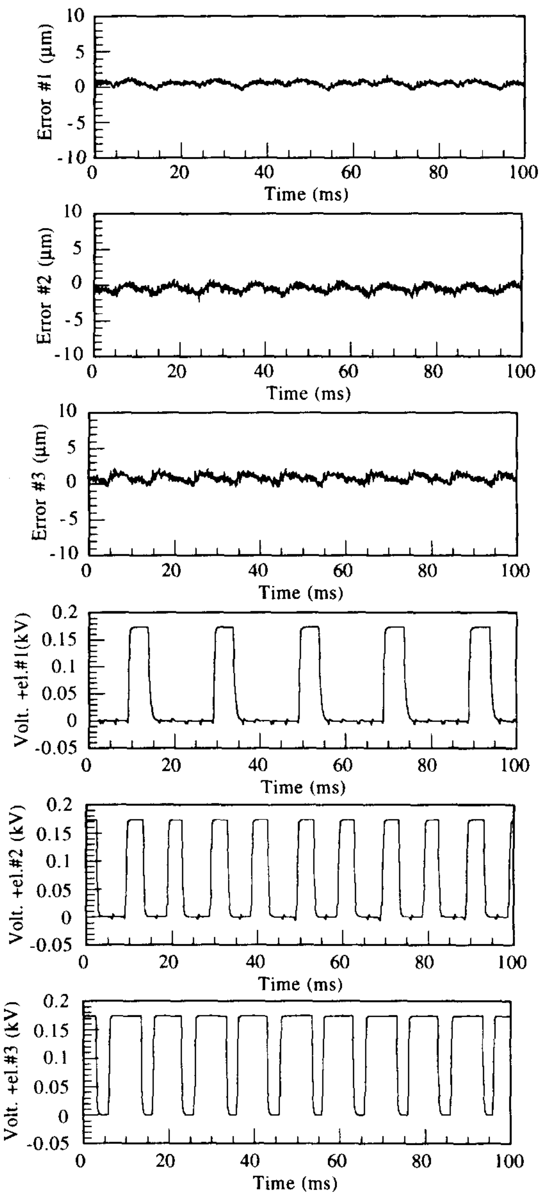

Fig. 7. Measured error signals and positively charged electrode voltage variations.

airgap at the three sensor sites and the electrode voltages V^+ of the inner electrodes which were charged to a $+V_{on}$ of +180 V.

As can be seen from Fig. 7, the wafer position showed a stable limit cycle at steady state in the form of a sustained oscillation around the reference position. Fig. 8 depicts a photograph of the wafer in a stably suspended state. It was verified that the measured airgap variations, which were all less than 1 μm, were of the same order as

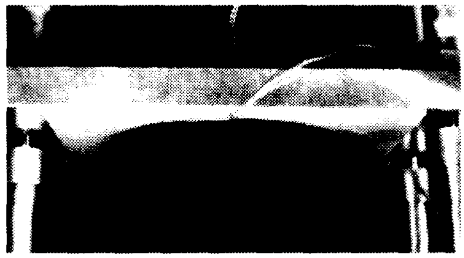

Fig. 8. Photograph showing rotor under stable suspension.

the sensor noise justifying the conclusion that the actual variations were very small. The reason for this lies in the fact that the squeeze film damping increases strongly for decreasing airgap lengths. The frequencies of the electrode voltages V^+ at the electrode units #1, #2, and #3 are approximately 50 Hz, 100 Hz, and 100 Hz, respectively. These frequencies correspond to those of the AC power supply and the ceiling lights and are a clear indication for the noise level in the measured airgaps.

6. CONCLUSIONS

A 4-inch silicon wafer was successfully levitated electrostatically using a newly developed switched-voltage control method which does not deploy any high-voltage amplifiers and is structurally highly simple. Therefore, the proposed method provides major improvements from economic, weight, space, and reliability points of view. Experimental validation of the proposed scheme has been performed through the successful suspension of a 4-inch silicon wafer at an airgap of 50 μm. It is shown that despite the inherent limit cycle property of relay feedback based control, an excellent performance in vibration suppression is attained due to the presence of a relatively large squeeze film damping.

A great advantage of this scheme is that the practical realization of large scale distributed electrode-sensor systems is made possible since the cost and size will be reduced substantially in comparison with the conventional systems that are based on high-voltage amplifiers and PID feedback control.

REFERENCES

[1] J. Jin, T. Higuchi and M. Kanemoto, "Electrostatic Silicon Wafer Suspension", *Proc. 4th Int. Symp. Magnetic Bearings*, ETH Zurich, Switzerland, pp. 343-348, August 1994.

[2] J. Jin, T. Higuchi and M. Kanemoto, "Electrostatic Levitator for Hard Disk Media", *IEEE Trans. Industrial Electronics*, Vol. 42, No. 5, pp. 467-473, 1995.

[3] J. U. Jeon, S. J. Woo and T. Higuchi, "Electrostatic Suspension of Glass Plate", *Proc. '96 Korea Automatic Control Conference*, Pohang, South-Korea, October 1996.

[4] J. U. Jeon, J. Jin and T. Higuchi, "Rotary Actuators with Electrostatic Suspension", *Proc. 5th Int. Symp. Magnetic Bearings*, Kanazawa, Japan, pp. 411-418, August 1996.

[5] S. J. Woo, J. U. Jeon, T. Higuchi and J. Jin, "Electrostatic Force Analysis of Electrostatic Levitation System", *Proc. 34th SICE Annual Conf.*, International Session, Hokkaido, Japan, pp. 1347-1352, July 1995.